

---

# Exploiting Expert-guided Symmetry Detection in Offline Reinforcement Learning

---

Giorgio Angelotti

Nicolas Drougard

Caroline P. C. Chanel

ANITI, University of Toulouse, France  
ISAE Supaero, University of Toulouse, France  
{name.surname}@isae-supaero.fr

## Abstract

Offline estimation of the dynamical model of a Markov Decision Process (MDP) is a non-trivial task that greatly depends on the data available to the learning phase. Sometimes the dynamics of the model is invariant with respect to some transformations of the current state and action. Recent works showed that an expert-guided pipeline relying on Density Estimation methods as Deep Neural Network based Normalizing Flows effectively detects this structure in deterministic environments, both categorical and continuous-valued. The acquired knowledge can be exploited to augment the original data set, leading eventually to a reduction in the distributional shift between the true and the learnt model. Such data augmentation technique can be exploited as a preliminary process to be executed before the adoption of an Offline Reinforcement Learning architecture, increasing its performance. In this work we extend the paradigm to also tackle non deterministic MDPs, in particular 1) we propose a detection threshold in categorical environments based on statistical distances, and 2) we show that the former results lead to a performance improvement when solving the learnt MDP and then applying the optimal policy in the real environment.

## 1 Introduction and Related Works

In Offline Reinforcement Learning (ORL) and Offline Learning for Planning the environment dynamics and/or value functions are inferred from a batch of already pre-collected experiences. Wrong previsions lead to bad decisions. The distributional shift, defined as the discrepancy between the learnt model and reality, is the main responsible for the performance deficit of the (sub)optimal policy obtained in the offline setting compared to the true optimal policy [1, 2]. Is there a way to exploit expert knowledge or intuition about the environment to limit the distributional shift? Several models benefit from a dynamics which is invariant with respect to some transformations of the system of reference. In physics, such a property of a system is called a symmetry [3]. In the context of Markov Decision Processes (MDPs) [4] a symmetry can be defined as a particular case of an MDP's homomorphism [5]. Knowing that a system to be learnt is endowed with a symmetry or of an homomorphic structure can lead to both more data- and computational- efficient solutions of an MDP.

The automatic discovery of homomorphic structures in MDPs has a long story [6–8]. In [9] a theoretical analysis of the possible types of MDPs state abstractions proved which properties of the original MDP would be invariant under the transformation: the optimal value function, the optimal policy, etc. Eventually, the full automatic discovery of a factored MDP representation was proven to be as hard as verifying whether two graphs are isomorphic [10]. In recent years [11, 12, 5] rekindled the topic. In the first work a contrastive loss function that enforces action equivariance on a to be learnt representation of an MDP was adopted to learn a structured latent space that was then

exploited to increase the data efficiency of a data-driven planner. In the second work MDP Invariant Networks, peculiar classes of Deep Neural Network (DNN) architectures that by construction enforce the invariance of the optimal MDP policy under some set of transformations obtained through other Deep RL paradigms, were introduced. The latter also provided an increase in data efficiency.

Recently [13] showed the importance of large and diverse datasets for ORL by demonstrating empirically that offline learning using a vanilla online RL algorithm over a batch that is diverse enough can lead to performances that are comparable to, or even better than, pure ORL approaches.

In [5] an expert-guided detection of alleged symmetries based on Density Estimation statistical techniques in the context of the offline learning of both continuous and categorical environments was proposed in order to eventually augment the starting data set. The authors showed that correctly detecting a symmetry and data augmenting the starting data set exploiting this information led to a decrease in the distributional shift. Unfortunately, the said work concerned only *deterministic* MDPs and did not include an analysis of the *performance* of the policy obtained in the end. In other fields of Machine Learning data augmentation has been extensively exploited to boost the efficiency of the algorithms in data-limited setups [14–16].

In this work we take over and extend the approach by also tackling stochastic environments. More specifically, the contributions of this paper are the followings:

1. A refinement of the decision threshold, based on statistical distances, is defined for categorical MDPs (also *stochastic*);
2. The improvement of the policy performance obtained by augmenting the data with the symmetric images of the transitions is demonstrated experimentally.

The presented method is not a competitor to the ORL algorithms, but a way to augment the batch by validating expert intuition. Once the batch has been augmented one could use any offline RL method.

## 2 Background

**Definition 1** (Markov Decision Process). An MDP [4] is a tuple  $\mathcal{M} = (S, A, R, T, \gamma)$ .  $S$  and  $A$  are the sets of states and actions,  $R : S \times A \rightarrow \mathbb{R}$  is the reward function,  $T : S \times A \rightarrow \text{Dist}(S)$  is the transition function, where  $\text{Dist}(S)$  is the set of probability distributions on  $S$ , and  $\gamma \in [0, 1]$  is the discount factor. Time is discretized and at each step  $t \in \mathbb{N}$  the agent observes a system state  $s = s_t \in S$ , acts with  $a = a_t \in A$  drawn from a policy  $\pi : S \rightarrow \text{Dist}(A)$ , and with probability  $T(s, a, s')$  transits to a next state  $s' = s_{t+1}$ , earning a reward  $R(s, a)$ . The value function of  $\pi$  and  $s$  is defined as the expected total discounted reward using  $\pi$  and starting with  $s$ :  $V_\pi(s) = \mathbb{E}_\pi[\sum_{t=0}^{\infty} \gamma^t R(s_t, a_t) | s_0 = s]$ . The optimal value function  $V^*$  is the maximum of the latter over every policy  $\pi$ .

**Definition 2** (MDP Symmetry). Given an MDP  $\mathcal{M}$ , let  $k$  be a surjection on  $S \times A \times S$  such that  $k(s, a, s') = (k_\sigma(s, a, s'), k_\alpha(s, a, s'), k_{\sigma'}(s, a, s')) \in S \times A \times S$ . Let  $(T \circ k)(s, a, s') = T(k_\sigma(s, a, s'))$ . Let  $k$  is a symmetry if  $\forall (s, s') \in S^2, a \in A$  both  $T$  and  $R$  are invariant with respect to the image of  $k$ :

$$(T \circ k)(s, a, s') = T(s, a, s'), \quad (1)$$

$$R(k_\sigma(s, a, s'), k_\alpha(s, a, s')) = R(s, a). \quad (2)$$

As in [5] we will focus only on the invariance of  $T$ , therefore we will only demand for the validity of Equation 1. Problems with a known reward function as well as model based approaches can thus benefit directly from the method.

**Probability Mass Function Estimation for Discrete MDPs.** Let  $\mathcal{D} = \{(s_i, a_i, s'_i)\}_{i=1}^n$  be a batch of recorded transitions. Performing mass estimation over  $\mathcal{D}$  amounts to compute the probabilities that define the categorical distribution  $T$  by estimating the frequencies of transition in  $\mathcal{D}$ . In other words:

$$\hat{T}(s, a, s') = \begin{cases} \frac{n_{s,a,s'}}{\sum_{s'} n_{s,a,s'}} & \text{if } \sum_{s'} n_{s,a,s'} > 0, \\ |S|^{-1} & \text{otherwise.} \end{cases} \quad (3)$$

where  $n_{s,a,s'}$  is the number of times the transition  $(s_t = s, a_t = a, s_{t+1} = s')$  appears in  $\mathcal{D}$ .

**Probability Density Function Estimation for Continuous MDPs.** Performing density estimation over  $\mathcal{D}$  means obtaining an analytical expression for the probability density function (pdf) of transitions  $(s, a, s')$  given  $\mathcal{D}$ :  $\mathcal{L}(s, a, s'|\mathcal{D})$ . Normalizing flows [17, 18] allow defining a parametric flow of continuous transformations that reshapes a known initial pdf to one that best fits the data.

**Expert-guided detection of symmetries** The paradigm described in [5] can be resumed as follows:

1. An expert presumes that a to be learnt model is endowed with the invariance of  $T$  with respect to a transformation  $k$ ;
2. (in the categorical case) He computes  $\hat{T}$ , an estimate of  $T$ , using the transitions in a batch  $\mathcal{D}$  by applying Equation 3;
3. (in the continuous case) He performs Density Estimation over  $\mathcal{D}$  using Normalizing Flows;
4. He applies  $k$  to all transitions  $(s, a, s') \in \mathcal{D}$  and then checks whether the fraction  $\nu_k$ 
  - (a) (categorical case) of samples  $k(s, a, s') = (k_\sigma(s, a, s'), k_\alpha(s, a, s'), k_{\sigma'}(s, a, s')) \in k(\mathcal{D})$  s.t.  $T(s, a, s') = (T \circ k)(s, a, s')$  exceeds an expert given threshold  $\nu$ ;
  - (b) (continuous case) of probability values  $\mathcal{L}$  evaluated on  $k(\mathcal{D})$  exceeds a threshold  $\theta$  that corresponds to the  $q$ -order quantile of the distribution of probability values evaluated on the original batch. The quantile order  $q$  is given as an input to the procedure by an expert (see Algorithm 2);
5. If the last condition is fulfilled then  $\mathcal{D}$  is augmented with  $k(\mathcal{D})$ .

Note that once a transformation  $k$  is detected as a symmetry the dataset is potentially augmented with transitions that are not present in the original batch, injecting hence unseen and totally novel information into the dataset.

### 3 Algorithmic Contribution

In this section we present the algorithmic contribution proposed in our work that improve the detection of alleged symmetries and its subsequent evaluation in *stochastic* MDPs.

#### 3.1 $\nu_k$ in the categorical setting

Our first contribution relies in the improvement of the calculation of  $\nu_k$  in part (4.a) of the previous list. Indeed, that approach does not yield valid results when applied to stochastic environments. In order for the method to work in stochastic environments we need to measure a distance in distribution. The latter somehow was already considered in the version of the approach that took care of continuous environments since learning a distribution over transitions represented by their features is independent of the typology of the dynamics. However, when dealing with categorical states the notion of distance between features can't be exploited.

We propose to compute the percentage  $\nu_k$  relying on a distance between categorical distributions. Since the transformation  $k$  is a surjection on transition tuples, we do not know a-priori which will be the correct mapping  $k_{\sigma'}(s, a, s') \forall s' \in S$ . In other words, we can compute  $k_{\sigma'}$ , the symmetric image of  $s'$ , only when we receive as an input the whole tuple  $(s, a, s')$  since an inverse mapping might not exist.

Therefore we will resort to compute a *pessimistic* approximation of the Total Variational Distance (proportional to the  $L^1$ -norm). In particular, given  $(s, a, s')$ , we aim to calculate the Chebyshev distance (the  $L^\infty$ -norm) between  $T(s, a, \cdot)$  and  $T(k_\sigma(s, a, s'), k_\alpha(s, a, s'), \cdot)$ . Recall that given two vectors of dimension  $d$ ,  $x$  and  $y$  both  $\in \mathbb{R}^d$ ,  $\|x - y\|_\infty \leq \|x - y\|_1$ .

Let us then define the following four functions:

$$\begin{aligned}
 m(s, a, s') &= \min_{\bar{s} \in S \setminus \{s'\} : \hat{T} \neq 0} \hat{T}(s, a, \bar{s}), & M(s, a, s') &= \max_{\bar{s} \in S \setminus \{s'\}} \hat{T}(s, a, \bar{s}), \\
 m_k(s, a, s') &= \min_{\substack{\bar{s} \in S \text{ s.t.} \\ \bar{s} \neq k_{\sigma'}(s, a, s') \\ \text{and } \hat{T} \circ k \neq 0}} \hat{T}(k_\sigma(s, a, s'), k_\alpha(s, a, s'), \bar{s}),
 \end{aligned}$$

$$M_k(s, a, s') = \max_{\substack{\bar{s} \in S \text{ s.t.} \\ \bar{s} \neq k_{\sigma'}(s, a, s')}} \hat{T}(k_{\sigma}(s, a, s'), k_{\alpha}(s, a, s'), \bar{s})$$

where  $m(M)$  and  $m_k(M_k)$  are the minimum (maximum) of the pmf  $\hat{T}$  when evaluated respectively on an initial state and action  $(s, a)$  and  $(k_{\sigma}(s, a, s'), k_{\alpha}(s, a, s'))$  for which  $\hat{T} \neq 0$  (those values are excluded because in the context of a small dataset, many transitions are unexplored and including values = 0 would often lead to too pessimistic estimates).

In order to approximate the Chebyshev distance between  $\hat{T}(s, a, \cdot)$  and  $\hat{T}(k_{\sigma}(s, a, s'), k_{\alpha}(s, a, s'), \cdot)$  we define a pessimistic approximation  $d_k$  as follows:

$$d_k(s, a, s') = \max \left\{ \underbrace{|M(s, a, s') - m_k(s, a, s')|}_{(I)}, \underbrace{|M_k(s, a, s') - m(s, a, s')|}_{(II)}, \underbrace{|\hat{T}(s, a, s') - (\hat{T} \circ k)(s, a, s')|}_{(III)} \right\}. \quad (4)$$

For the moment consider  $\hat{T}(s, a, \cdot)$  and  $\hat{T}(k_{\sigma}(s, a, s'), k_{\alpha}(s, a, s'), \cdot)$  just as two sets of numbers. Remove the value corresponding to  $s'$  from the first set, the one corresponding to  $k_{\sigma'}(s, a, s')$  from the second set and any remaining zeroes from both. Taking the max between (I) and (II) just equates to selecting the maximum possible difference between any two values of these modified sets. Equation 4 simply tells us to select the worst possible case since we do not know which permutations of states we should compare when computing the Chebyshev distance.  $s'$  is removed from  $\hat{T}(s, a, \cdot)$  and  $k_{\sigma'}(s, a, s')$  is removed from  $\hat{T}(k_{\sigma}(s, a, s'), k_{\alpha}(s, a, s'), \cdot)$  since we know that  $k$  maps  $(s, a, s')$  to  $(k_{\sigma}(s, a, s'), k_{\alpha}(s, a, s'), k_{\sigma'}(s, a, s'))$  and hence we can compare those values directly (III).

Notice that

$$0 < d_k(s, a, s') \leq 1 \quad \forall (s, a, s') \in S \times A \times S. \quad (5)$$

We propose then to estimate  $\nu_k$  as in Line 2 of Algorithm 1:

$$\nu_k(\mathcal{D}) = 1 - \frac{1}{|\mathcal{D}|} \sum_{(s, a, s') \in \mathcal{D}} d_k(s, a, s'). \quad (6)$$

From equations 4 and 5, it follows that 1) in deterministic environments  $\nu_k$  (Eq. 6) coincides with the one prescribed in [5] and 2)  $1 > \nu_k \geq 0$ , so  $\nu_k$  can be interpreted as a percentage. The last remark allows us to suppose that  $\nu_k$  is an estimate of the probability of  $k$  being a symmetry of the dynamics, and therefore we can relax the necessity of defining an expert-given threshold  $\nu$  as an input in Algorithm 1 by setting  $\nu = 0.5$  and eventually augmenting the batch if  $\nu_k > 0.5$  (Lines 3-5).

*Remark* (Extreme case scenario). Is Equation 4 too pessimistic? Consider that for a given state action couple  $(\bar{s}, \bar{a})$  we have a transition distributed over 3 states  $s \in S = \{One, Two, Three\}$  with probabilities  $T(\bar{s}, \bar{a}, One) = 0.01$ ,  $T(\bar{s}, \bar{a}, Two) = 0.01$  and  $T(\bar{s}, \bar{a}, Three) = 0.98$ . Now, assume the estimate of the transition function is perfect. Does the distance in Equation 4 converge to 0? Not always, but what matters for the detection of symmetries is the average of the distances over the whole batch (Eq. 6). Suppose that these probabilities were inferred from a batch with the transition  $(\bar{s}, \bar{a}, One)$  once,  $(\bar{s}, \bar{a}, Two)$  once and  $(\bar{s}, \bar{a}, Three)$  ninety-eight times. Consider  $(\bar{s}, \bar{a}, Three)$ .  $M(\bar{s}, \bar{a}, Three) = M_k(\bar{s}, \bar{a}, Three) = m(\bar{s}, \bar{a}, Three) = m_k(\bar{s}, \bar{a}, Three) = 0.01$ . Following Eq. 4,  $d_k(\bar{s}, \bar{a}, Three) = 0$ . However,  $d_k(\bar{s}, \bar{a}, One) = d_k(\bar{s}, \bar{a}, Two) = 0.97$ , which is a too pessimistic estimate. Nevertheless let's calculate  $\nu_k$  (Eq.6). For this state-action pair  $(\bar{s}, \bar{a})$ , the average over the batch is therefore:  $(d_k(\bar{s}, \bar{a}, One) + d_k(\bar{s}, \bar{a}, Two) + 98d_k(\bar{s}, \bar{a}, Three))/100 = 0.0194$ . If the estimation is the same for other pairs  $(s, a)$ , then  $\nu_k = 1 - 0.0194 = 0.9806$ . This is a value close to 1 suggesting  $k$  is a symmetry.

## 4 Experiments

In order to show the improvements provided by our contribution we tested the algorithms in a stochastic version of the toroidal Grid environment and two continuous state environments of the OpenAI's Gym Learning Suite: CartPole and Acrobot. The deterministic version of these environments were used for the experiments in [5] and so they make a valid set of scenarios to assess the validity of our approach.

---

**Algorithm 1:** Symmetry detection and data augmenting in a categorical MDP

---

**Input:** Batch of transitions  $\mathcal{D}$ ,  $k$  alleged symmetry**Output:** Possibly augmented batch  $\mathcal{D} \cup \mathcal{D}_k$ 

```
1  $\hat{T} \leftarrow$  Most Likely Categorical pmf from  $(\mathcal{D})$ 
2  $\nu_k = 1 - \frac{1}{|\mathcal{D}|} \sum_{(s,a,s') \in \mathcal{D}} d_k(s,a,s')$  (where  $d_k$  is defined in Equation 4)
3 if  $\nu_k > 0.5$  then
4   |  $\mathcal{D}_k = k(\mathcal{D})$  (batch of alleged symmetric transitions)
5   | return  $\mathcal{D} \cup \mathcal{D}_k$  (the augmented batch)
6 else
7   | return  $\mathcal{D}$  (the original batch)
8 end
```

---

---

**Algorithm 2:** Symmetry detection and data augmenting in a continuous MDP with detection threshold  $\nu = 0.5$  [5]

---

**Input:** Batch of transitions  $\mathcal{D}$ ,  $q \in [0, 1)$  order of the quantile,  $k$  alleged symmetry**Output:** Possibly augmented batch  $\mathcal{D} \cup \mathcal{D}_k$ 

```
1  $\mathcal{L} \leftarrow$  Density Estimate  $(\mathcal{D})$  (e.g. with Normalizing Flows)
2  $\Lambda \leftarrow$  Distribution  $\mathcal{L}(\mathcal{D})$  ( $\mathcal{L}$  evaluated over  $\mathcal{D}$ )
3  $\theta = q$ -order quantile of  $\Lambda$ 
4  $\mathcal{D}_k = k(\mathcal{D})$  (batch of alleged symmetric transitions)
5  $\nu_k = \frac{1}{|\mathcal{D}_k|} \sum_{(s,a,s') \in \mathcal{D}_k} \mathbb{1}_{\{\mathcal{L}(s,a,s'|\mathcal{D}) > \theta\}}$ 
6 if  $\nu_k > 0.5$  then
7   | return  $\mathcal{D} \cup \mathcal{D}_k$  (the augmented batch)
8 else
9   | return  $\mathcal{D}$  (the original batch)
10 end
```

---

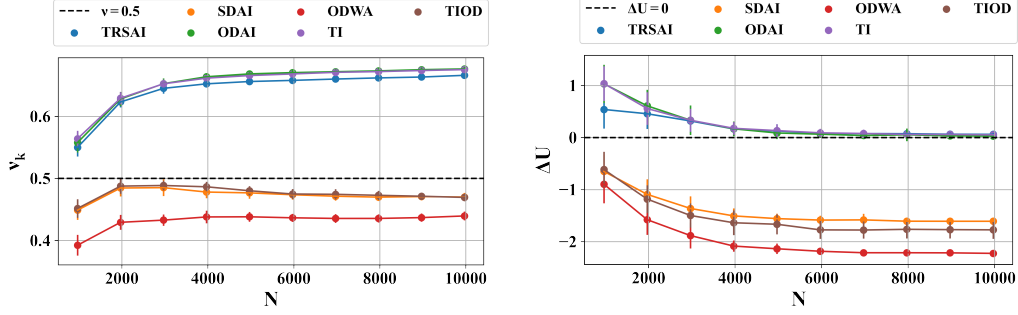
#### 4.1 Setup

We collect a batch of transitions  $\mathcal{D}$  using a uniform random policy. An expert alleges the presence of a symmetry  $k$  and we proceed to its detection using Algorithm 1 (categorical case) or Algorithm 2 (continuous case). In the continuous case Density Estimation is performed by a Masked Autoregressive Flow architecture [19] with 3 layers of bijectors.

The experiments were performed using 2 Dodeca-core Skylake Intel® Xeon® Gold 6126 @ 2.6 GHz and 96 GB of RAM and 2 GPU NVIDIA® V100 @ 192GB of RAM. The code to run the experiments is available at <https://github.com/giorgioangel/dsym>.

**Computation of  $\nu_k$  and batch augmentation** We report the  $\nu_k$  obtained with an ensemble of  $N$  different iterations of the procedure: we generate  $z \in \mathbb{N}$  sets of  $N$  different batches  $\mathcal{D}$  of increasing size (in the original paper only one batch size was considered). Remember that since  $\nu_k \in [0, 1)$  we can interpret it as the probability of the presence of a symmetry and select a detection threshold  $\nu = 0.5$ , while in [5] the threshold  $\nu$  was expert-given.

**Evaluation of the performance (Categorical case)** In the end, let  $\rho$  be the distribution of initial states  $s_0 \in S$  and let the performance  $U^\pi$  of a policy  $\pi$  be  $U^\pi = \mathbb{E}_{s \sim \rho}[V^\pi(s)]$ . our final contribution is the comparison between the performances obtaining by acting in the real environment with  $\hat{\pi}$  (the optimal policy obtained by solving the MDP learnt with  $\hat{T}$ ) and  $\hat{\pi}_k$  (the optimal policy obtained with  $\hat{T}_k$ ). In particular we consider the quantity  $\Delta U = U^{\hat{\pi}_k} - U^{\hat{\pi}}$ . In *categorical* environments the policies are obtained with Policy Iteration and evaluated with Policy Evaluation.



(a) Probability of symmetry  $\nu_k$ . The threshold at  $\nu = 0.5$  is displayed as a dashed line.  $\nu_k > 0.5$  means that the transformation is detected as a symmetry.

(b) Performance difference  $\Delta U$ . The threshold at  $\Delta U = 0$  is displayed as a dashed line.  $\Delta U > 0$  means that data augmenting leads to better policies.

Figure 1: Stochastic toroidal Grid Environment.  $\nu_k$  and  $\Delta U$  for the transformations  $k$  computed over sets of 100 different batches of size  $N$ . Points are mean values and bars standard deviations.

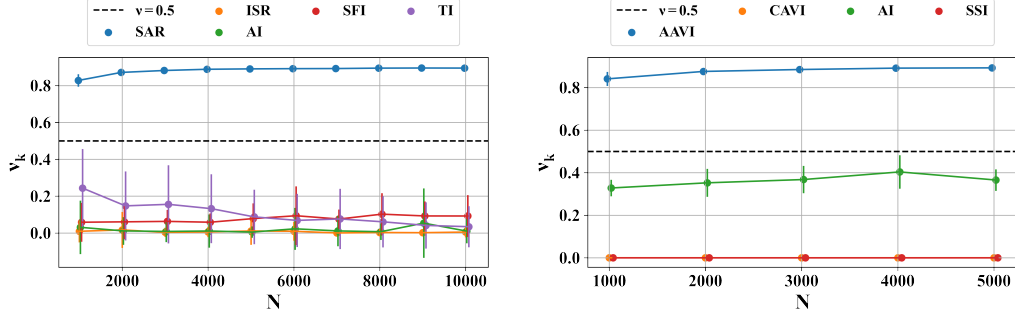
**Evaluation of the performance (Continuous case)** In *continuous* environments Offline Learning is not trivial. We use the implementation of two Model-Free Deep RL architectures: Deep Q-Network (DQN) [20] and Conservative Q-Learning (CQL) [21] of the d3rlpy learning suite [22] to obtain a policy starting from the batches. The first method is the one that originally established the validity of Deep RL and it is used in online RL while the second was specifically developed to tackle offline problems. Since the convergence of the training of Deep RL baselines is greatly dependent of hyperparameter tuning that itself depends on both the environment and the batch [23], we will apply DQN and CQL with the default parameters provided by d3rlpy, abiding hence more faithfully to an offline learning duty. This means that sometimes the learning might not converge to a good policy. We find this philosophy more honest than showing the results obtained with the best seed or the finest-tuned hyperparameters. Each architecture is trained for a number of steps equal to fifty times the number of transitions present in the batch.

## 4.2 Environments

Table 1: Grid. Proposed transformations and label.

| $k$                                                                                                                                                                                                                                                                                      | Label |
|------------------------------------------------------------------------------------------------------------------------------------------------------------------------------------------------------------------------------------------------------------------------------------------|-------|
| $k_\sigma(s, a, s') = s'$<br>$k_\alpha(s, a = (\uparrow, \downarrow, \leftarrow, \rightarrow), s') = (\downarrow, \uparrow, \rightarrow, \leftarrow)$<br>$k_{\sigma'}(s, a, s') = s$                                                                                                     | TRSAI |
| $k_\sigma(s, a, s') = s$<br>$k_\alpha(s, a = (\uparrow, \downarrow, \leftarrow, \rightarrow), s') = (\downarrow, \uparrow, \rightarrow, \leftarrow)$<br>$k_{\sigma'}(s, a, s') = s'$                                                                                                     | SDAI  |
| $k_\sigma(s, a, s') = s$<br>$k_\alpha(s, a = (\uparrow, \downarrow, \leftarrow, \rightarrow), s') = (\downarrow, \uparrow, \rightarrow, \leftarrow)$<br>$k_{\sigma'}(s, a = (\uparrow, \downarrow, \leftarrow, \rightarrow), s') = (s' - (0, 2), s' + (0, 2), s' + (2, 0), s' - (2, 0))$ | ODAI  |
| $k_\sigma(s, a, s') = s$<br>$k_\alpha(s, a = (\uparrow, \downarrow, \leftarrow, \rightarrow), s') = (\rightarrow, \leftarrow, \uparrow, \downarrow)$<br>$k_{\sigma'}(s, a = (\uparrow, \downarrow, \leftarrow, \rightarrow), s') = (s' - (0, 2), s' + (0, 2), s' + (2, 0), s' - (2, 0))$ | ODWA  |
| $k_\sigma(s, a, s') = s'$<br>$k_\alpha(s, a, s') = a$<br>$k_{\sigma'}(s, a = (\uparrow, \downarrow, \leftarrow, \rightarrow), s') = (s' + (0, 1), s' - (0, 1), s' - (1, 0), s' + (1, 0))$                                                                                                | TI    |
| $k_\sigma(s, a, s') = s'$<br>$k_\alpha(s, a, s') = a$<br>$k_{\sigma'}(s, a, s') = s$                                                                                                                                                                                                     | TIOD  |

**Stochastic Grid (Categorical)** In this environment the agent can move along fixed directions over a torus by acting with any  $a \in A = \{\uparrow, \downarrow, \leftarrow, \rightarrow\}$ . The grid meshing the torus has size  $l = 10$ . The agent can spawn everywhere on the torus with a uniform probability and must reach a fixed goal. At every time step he receives a reward  $r = -1$  if he does not reach the goal and a reward  $r = 1$  once



(a) Stochastic CartPole. Probability of symmetry  $\nu_k$ . The threshold at  $\nu = 0.5$  is displayed as a dashed line.  $\nu_k > 0.5$  means that the transformation is detected as a symmetry.

(b) Stochastic Acrobot. Probability of symmetry  $\nu_k$ . The threshold at  $\nu = 0.5$  is displayed as a dashed line.  $\nu_k > 0$  means that the transformation is detected as a symmetry.

Figure 2:  $\nu_k$ , for the transformations  $k$  computed over sets of different batches of size  $N$  in Stochastic CartPole (left) and Stochastic Acrobot (right). Points are mean values and are a bit shifted horizontally for the sake of display. Standard deviation is displayed as a vertical error bar.

the goal has been reached, terminating the episode. When performing an action the agent has 60% chances of moving to the intended direction, 20% to the opposite one, and 10% along an orthogonal direction. We collect  $z = 10$  sets of  $M = 100$  batches with respectively  $N = 1000 \times i_z$  steps in each batch ( $i_z$  going from 1 to  $z$ ). The proposed symmetries for this environment are outlined in Table 1. We check for the invariance of the dynamics with respect to the following six transformations (the valid symmetries are displayed in **bold**): 1) Time reversal symmetry with action inversion (**TRSAI**); 2) Same dynamics with action inversion (**SDAI**); 3) Opposite dynamics and action inversion (**ODAI**); 4) Opposite dynamics but wrong action (**ODWA**); 5) Translation invariance (**TI**); 6) Translation invariance with opposite dynamics (**TIOD**). The  $N$  dependent average results are reported in Figure 1 along with the standard deviation represented by a vertical error bar.

**Stochastic CartPole (Continuous)** The dynamics is similar to that of CartPole [24], however the force that the agent uses to push the cart is sampled from a normal distribution with mean  $f$  (the force defined in the deterministic version) and standard deviation  $\tilde{\sigma} = 2$ . Recall that the state is represented by the features  $(x, \theta, v, \omega)$  and  $A = \{\leftarrow, \rightarrow\}$ . For the evaluation of  $\nu_k$  we set the quantile  $q = 0.1$  and we collect  $z = 10$  sets of  $M = 100$  batches with respectively  $N = 1000 \times i_z$  steps in each batch (and  $i_z$  going from 1 to 10). We evaluate  $\Delta U$  by training the agent on single batches of  $N = 5000 \times i_z$  (and  $i_z$  going from 1 to 6) both augmented and not augmented with  $k$ . The acronyms of the valid symmetric transformations are displayed in **bold**: 1) State and action reflection with respect to an axis in  $x = 0$  (**SAR**); 2) Initial state reflection (**ISR**); 3) Action inversion (**AI**); 4) Single feature inversion (**SFI**); 5) Translation invariance (**TI**). Their effects on the transition  $(s, a, s')$  are listed in Table 2. Average results and errors are displayed in Figure 2.

**Stochastic Acrobot (Continuous)** It is the very same Acrobot of [24] but at every time step a noise  $\epsilon$  is sampled from an uniform distribution on the interval  $[-0.5, 0.5]$  and added to the torque. A state is represented by the features  $(s_1, c_1, s_2, c_2, \omega_1, \omega_2)$  where  $s_i$  and  $c_i$  are respectively  $\sin(\alpha_i)$  and  $\cos(\alpha_i)$  in shorthand notation. The action set  $A = \{-1, 0, 1\}$ . For the evaluation of  $\nu_k$  we set  $q = 0.1$ . For the detection case we collected  $z = 5$  sets of  $M = 100$  batches with  $N = 1000 \times i_z$  steps within each one ( $i_z$  going from 1 to  $z$ ). The evaluation of the performance was carried out on single batches, with and without data augmentation, with  $N = 10000 \times i_z$  steps and  $i_z$  going from 1 to 4. For the evaluation of  $\Delta z = 5$  due to computational necessities. We allege the following transformations  $k$ , as always the valid ones are **bolded**: 1) Angles and angular velocities inversion (**AAVI**); 2) Cosines and angular velocities inversion (**CAVI**); 3) Action inversion (**AI**); 4) Starting state inversion (**SSI**). The images of the transformations are reported in Table 2. The  $N$  dependent average results and standard deviations are reported in Figure 2.

Table 2: Proposed transformations and labels for Stochastic CartPole (left) and Stochastic Acrobot (right).

| $k$                                                                          | Label      | $k$                                                                 | Label       |
|------------------------------------------------------------------------------|------------|---------------------------------------------------------------------|-------------|
| $k_\sigma(s, a, s') = -s$                                                    | <b>SAR</b> | $k_\sigma(s = (s_1, s_2, \omega_1, \omega_2, \dots), a, s')$        | <b>AAVI</b> |
| $k_\alpha(s, a = (\leftarrow, \rightarrow), s') = (\rightarrow, \leftarrow)$ |            | $= (-s_1, -s_2, -\omega_1, -\omega_2, \dots)$                       |             |
| $k_{\sigma'}(s, a, s') = -s'$                                                |            | $k_\alpha(s, a = (-1, 0, 1), s') = (1, 0, -1)$                      |             |
| $k_\sigma(s, a, s') = -s$                                                    | <b>ISR</b> | $k_{\sigma'}(s, a, s' = (s'_1, s'_2, \omega'_1, \omega'_2, \dots))$ | <b>CAVI</b> |
| $k_\alpha(s, a, s') = a$                                                     |            | $= (-s'_1, -s'_2, -\omega'_1, -\omega'_2, \dots)$                   |             |
| $k_{\sigma'}(s, a, s') = s'$                                                 |            | $k_\sigma(s = (c_1, c_2, \omega_1, \omega_2, \dots), a, s')$        | <b>AI</b>   |
| $k_\sigma(s, a, s') = s$                                                     | <b>AI</b>  | $= (-c_1, -c_2, -\omega_1, -\omega_2, \dots)$                       |             |
| $k_\alpha(s, a = (\leftarrow, \rightarrow), s') = (\rightarrow, \leftarrow)$ |            | $k_\alpha(s, a = (-1, 0, 1), s') = (1, 0, -1)$                      |             |
| $k_{\sigma'}(s, a, s') = s'$                                                 | <b>SFI</b> | $k_{\sigma'}(s, a, s' = (c'_1, c'_2, \omega'_1, \omega'_2, \dots))$ | <b>SSI</b>  |
| $k_\sigma(s = (x, \dots), a, s') = (-x, \dots)$                              |            | $= (-c'_1, -c'_2, -\omega'_1, -\omega'_2, \dots)$                   |             |
| $k_\alpha(s, a, s') = a$                                                     |            | $k_\sigma(s, a, s') = s$                                            | <b>AI</b>   |
| $k_{\sigma'}(s, a, s') = s'$                                                 | <b>TI</b>  | $k_\alpha(s, a = (-1, 0, 1), s') = (1, 0, -1)$                      |             |
| $k_\sigma(s = (x, \dots), a, s') = (x + 0.3, \dots)$                         |            | $k_{\sigma'}(s, a, s') = s'$                                        |             |
| $k_\alpha(s, a, s') = a$                                                     | <b>TI</b>  | $k_\sigma(s, a, s') = -s$                                           | <b>SSI</b>  |
| $k_{\sigma'}(s, a, s' = (x', \dots)) = (x' + 0.3, \dots)$                    |            | $k_\alpha(s, a, s') = a$                                            |             |
|                                                                              |            | $k_{\sigma'}(s, a, s') = s'$                                        |             |

## 5 Discussion

**Stochastic Grid (Categorical) - Detection phase ( $\nu_k$ )** In Grid the algorithm perfectly manages to identify the real symmetries of the environment:  $\nu_k > 0.5$ ,  $k \in \{TRSAI, ODAI, TI\}$ . Moreover, there are no false positives:  $\nu_k < 0.5$ ,  $k \in \{SDAI, ODWA, TIOD\}$ . We notice that while in a deterministic environment  $\nu_k = 0 \forall k$  which is not a symmetry, here the stochasticity makes the detection more complicated since  $\nu_k \approx 0.5^-$  for  $N = 2000$ .

**Stochastic Grid (Categorical) - Evaluation of performance gain ( $\Delta U$ )** The difference in performance of the deployed policies  $\Delta U$  perfectly fits the expected behaviour. When  $k$  is a symmetry  $\Delta U > 0$  and saturates to 0 with  $N$  increasing. When  $k$  is not a symmetric transformation of the dynamics  $\Delta U < 0$  and keeps decreasing with  $N$  (see Figure 1b).

**Stochastic CartPole (Continuous) - Detection phase ( $\nu_k$ )** In Stochastic CartPole the algorithm fails to detect the symmetry  $k = TI$ . This could be due to the fact that the translation invariance symmetry in this case is fixed for a specific value (see TI in Table 2 where the translation is set at 0.3). If the translation is too small the neural network fails to discern the transformation from the noise. The algorithm classifies correctly as a symmetry  $k = SAR$  and the remaining transformations as non symmetries (see Figure 2a).

**Stochastic CartPole (Continuous) - Evaluation of performance gain ( $\Delta U$ )** Results are displayed in Table 3. ORL is very unstable and sensitive to the choice of hyperparameters. On top of that the training is carried out for a fixed number of epochs. We notice that, on average over different batch sizes,  $\Delta U > 0$  for DQN and SAR and SFI. While SAR is a valid symmetry, SFI it's not. A more conservative algorithm like CQL only detects SAR as a valid symmetry. The performance difference for TI both for DQN and CQL is so close to zero that we think that augmenting the dataset with this symmetry might not be a substantial power up over using just the information contained in the original batch.

**Stochastic Acrobot (Continuous) - Detection phase ( $\nu_k$ )** In this environment the only real symmetry of the dynamics, AAVI, gets successfully detected by the algorithm with  $q = 0.1$ . Non symmetries yield a  $\nu_k < 0.5$  (Figure 2).

**Stochastic Acrobot (Continuous) - Evaluation of performance gain ( $\Delta U$ )** Results are displayed in Table 4 and show that the training in Stochastic Acrobot is harder than in Stochastic CartPole since, even with a large dataset, sometimes the algorithms do not manage to learn a good policy.



Table 3:  $\Delta U$  for every alleged symmetry in Stochastic CartPole with two baselines and different batch sizes  $N$ .

| $k$ | Baseline   | $N$ (number of transitions in the original batch) |       |       |       |        |       | Average |
|-----|------------|---------------------------------------------------|-------|-------|-------|--------|-------|---------|
|     |            | 5000                                              | 10000 | 15000 | 20000 | 25000  | 30000 |         |
| SAR | <i>DQN</i> | -7.3                                              | 25.4  | 41.8  | 7.2   | 9.0    | 3.4   | 13.3    |
|     | <i>CQL</i> | 37.4                                              | -2.5  | -4.1  | 20.1  | 17.9   | -9.0  | 10.0    |
| ISR | <i>DQN</i> | -1.3                                              | -48.5 | -29.9 | -78.7 | -107.8 | -29.1 | -49.2   |
|     | <i>CQL</i> | 6.4                                               | 1.6   | -2.2  | -22.3 | -10.3  | -25.9 | -8.8    |
| AI  | <i>DQN</i> | 26.9                                              | -48.5 | -43.7 | -74.6 | -41.3  | -84.6 | -44.3   |
|     | <i>CQL</i> | -13.1                                             | -7.6  | -29.8 | -6.5  | -22.3  | -15.3 | -15.8   |
| SFI | <i>DQN</i> | -33.4                                             | 17.9  | 21.4  | 45.4  | -6.9   | -0.1  | 7.4     |
|     | <i>CQL</i> | -5.5                                              | -2.1  | 7.4   | -3.9  | -3.6   | -18.5 | -4.4    |
| TI  | <i>DQN</i> | 36.9                                              | -28.1 | 34.5  | 15.7  | 6.1    | -9.1  | -0.2    |
|     | <i>CQL</i> | 7.6                                               | -1.3  | -2.1  | 11.8  | -16.5  | 5.2   | 0.8     |

Table 4:  $\Delta U$  for every alleged symmetry in Stochastic Acrobot with two baselines and different batch sizes  $N$ .

| $k$  | Baseline   | $N$ (number of transitions in the original batch) |        |        |        |  | Average |
|------|------------|---------------------------------------------------|--------|--------|--------|--|---------|
|      |            | 10000                                             | 20000  | 30000  | 40000  |  |         |
| AAVI | <i>DQN</i> | 24.7                                              | -17.5  | -63.4  | -10.6  |  | -16.7   |
|      | <i>CQL</i> | -2.8                                              | 10.5   | -9.5   | 213.3  |  | 52.9    |
| CAVI | <i>DQN</i> | 8.9                                               | -9.3   | -24.6  | -48.0  |  | -12.2   |
|      | <i>CQL</i> | -8.8                                              | 0.5    | 4.4    | 1.1    |  | -0.7    |
| AI   | <i>DQN</i> | -377.3                                            | -399.3 | -386.8 | -388.5 |  | -388.0  |
|      | <i>CQL</i> | -25.6                                             | 235.3  | -88.2  | -49.9  |  | 17.9    |
| SSI  | <i>DQN</i> | 265.7                                             | -408.2 | -334.9 | -396.3 |  | -218.4  |
|      | <i>CQL</i> | 35.8                                              | 4.0    | 11.9   | -22.8  |  | 7.2     |

In particular, while CQL manages to learn how to behave in the environment exploiting the AAVI symmetry (average  $\Delta U = 52.9$ ), DQN still struggles with every  $k$ , good and wrong. Nevertheless, CQL apparently benefits from augmenting the dataset also with wrong symmetries even though at a smaller extent. We suppose this effect is due to the instability in ORL training.

## 6 Conclusions

Data-efficiency in the offline learning of data-driven MDPs is highly coveted. Exploiting the intuition of an expert about the nature of the model can help to learn dynamics that better represent the reality. In this work we built a semi-automated tool that can aid an expert providing a statistical data-driven validation of his intuition about some properties of the environment. A correct deployment of the tool could improve the performance of the optimal policy obtained by solving the learnt MDP. Indeed, our results suggest that the proposed algorithm can effectively detect a symmetry of the dynamics of an MDP with high accuracy and that exploiting this knowledge can not only reduce the distributional shift, but also provide performance gain in an envisaged optimal control of the system. However, when applied to ORL environments with DNN, all the prescriptions (and issues) about hyperparameter fine-tuning well known to ORL practitioners persist. Besides its pros, the current work is still constrained by several limitations: e.g. the quality of the approach in continuous MDPs is greatly affected by the architecture of the Normalizing Flow used for Density Estimation and, more generally, by the state-action space preprocessing. In the future we plan to expand this approach by trying out more recent Normalizing Flow architectures like FFJORD [25].

## Checklist

1. For all authors...
  - (a) Do the main claims made in the abstract and introduction accurately reflect the paper’s contributions and scope? [Yes]
  - (b) Did you describe the limitations of your work? [Yes] Limitations are described throughout the paper.
  - (c) Did you discuss any potential negative societal impacts of your work? [Yes] We say that misdetecting a symmetry can be detrimental to the policy.
  - (d) Have you read the ethics review guidelines and ensured that your paper conforms to them? [Yes]
2. If you are including theoretical results...
  - (a) Did you state the full set of assumptions of all theoretical results? [Yes] Section 3
  - (b) Did you include complete proofs of all theoretical results? [N/A]
3. If you ran experiments...
  - (a) Did you include the code, data, and instructions needed to reproduce the main experimental results (either in the supplemental material or as a URL)? [Yes] Github repository linked in Section 4.1
  - (b) Did you specify all the training details (e.g., data splits, hyperparameters, how they were chosen)? [Yes] Mainly in the main text and the rest in the Supplementary Material
  - (c) Did you report error bars (e.g., with respect to the random seed after running experiments multiple times)? [Yes] For the categorical case, (Figure 1) and for the detection of continuous symmetries (Figure 2)
  - (d) Did you include the total amount of compute and the type of resources used (e.g., type of GPUs, internal cluster, or cloud provider)? [Yes] Type of resource - Section 4.1
4. If you are using existing assets (e.g., code, data, models) or curating/releasing new assets...
  - (a) If your work uses existing assets, did you cite the creators? [N/A]
  - (b) Did you mention the license of the assets? [N/A]
  - (c) Did you include any new assets either in the supplemental material or as a URL? [N/A]
  - (d) Did you discuss whether and how consent was obtained from people whose data you’re using/curating? [N/A]
  - (e) Did you discuss whether the data you are using/curating contains personally identifiable information or offensive content? [N/A]
5. If you used crowdsourcing or conducted research with human subjects...
  - (a) Did you include the full text of instructions given to participants and screenshots, if applicable? [N/A]
  - (b) Did you describe any potential participant risks, with links to Institutional Review Board (IRB) approvals, if applicable? [N/A]
  - (c) Did you include the estimated hourly wage paid to participants and the total amount spent on participant compensation? [N/A]

## References

- [1] Sergey Levine, Aviral Kumar, G. Tucker, and Justin Fu. Offline reinforcement learning: Tutorial, review, and perspectives on open problems. *ArXiv*, abs/2005.01643, 2020.
- [2] Giorgio Angelotti, Nicolas Drougare, and Caroline Ponzoni Carvalho Chanel. Offline learning for planning: A summary. In *Proceedings of the 1st Workshop on Bridging the Gap Between AI Planning and Reinforcement Learning (PRL) at the 30th International Conference on Automated Planning and Scheduling*, pages 153–161, 2020.
- [3] David J. Gross. The role of symmetry in fundamental physics. *Proceedings of the National Academy of Sciences*, 93(25):14256–14259, 1996. ISSN 0027-8424. doi: 10.1073/pnas.93.25.14256. URL <https://www.pnas.org/content/93/25/14256>.

- [4] Richard Bellman. Dynamic Programming. *Science*, 153(3731):34–37, 1966.
- [5] Giorgio Angelotti, Nicolas Drougard, and Caroline P. C. Chanel. Expert-guided symmetry detection in markov decision processes, 2021.
- [6] Thomas Dean and Robert Givan. Model Minimization in Markov Decision Processes. In *AAAI/IAAI*, pages 106–111, 1997.
- [7] B. Ravindran and A. G. Barto. Symmetries and Model Minimization in Markov Decision Processes. Technical report, USA, 2001.
- [8] Balaraman Ravindran and Andrew G Barto. Approximate Homomorphisms: A Framework for Non-exact Minimization in Markov Decision Processes. 2004.
- [9] Lihong Li, Thomas J Walsh, and Michael L Littman. Towards a Unified Theory of State Abstraction for MDPs. *ISAIM*, 4:5, 2006.
- [10] Shravan Matthur Narayanamurthy and Balaraman Ravindran. On the Hardness of Finding Symmetries in Markov Decision Processes. In *Proceedings of the 25th international conference on Machine learning*, pages 688–695, 2008.
- [11] Elise van der Pol, Thomas Kipf, Frans A. Oliehoek, and Max Welling. Plannable Approximations to MDP Homomorphisms: Equivariance under Actions. In *Proceedings of the 19th International Conference on Autonomous Agents and MultiAgent Systems*, AAMAS ’20, page 1431–1439, Richland, SC, 2020. International Foundation for Autonomous Agents and Multiagent Systems. ISBN 9781450375184.
- [12] Elise van der Pol, Daniel Worrall, Herke van Hoof, Frans Oliehoek, and Max Welling. MDP Homomorphic Networks: Group Symmetries in Reinforcement Learning. In H. Larochelle, M. Ranzato, R. Hadsell, M. F. Balcan, and H. Lin, editors, *Advances in Neural Information Processing Systems*, volume 33, pages 4199–4210. Curran Associates, Inc., 2020. URL <https://proceedings.neurips.cc/paper/2020/file/2be5f9c2e3620eb73c2972d7552b6cb5-Paper.pdf>.
- [13] Denis Yarats, David Brandfonbrener, Hao Liu, Michael Laskin, Pieter Abbeel, Alessandro Lazaric, and Lerrel Pinto. Don’t change the algorithm, change the data: Exploratory data for offline reinforcement learning. *arXiv preprint arXiv:2201.13425*, 2022.
- [14] David A van Dyk and Xiao-Li Meng. The art of data augmentation. *Journal of Computational and Graphical Statistics*, 10(1):1–50, 2001. doi: 10.1198/10618600152418584. URL <https://doi.org/10.1198/10618600152418584>.
- [15] Connor Shorten and Taghi M Khoshgoftaar. A survey on Image Data Augmentation for Deep Learning. *Journal of Big Data*, 6(1):1–48, 2019.
- [16] Daniel S Park, William Chan, Yu Zhang, Chung-Cheng Chiu, Barret Zoph, Ekin D Cubuk, and Quoc V Le. Specaugment: A simple data augmentation method for automatic speech recognition. *arXiv preprint arXiv:1904.08779*, 2019.
- [17] Laurent Dinh, David Krueger, and Yoshua Bengio. NICE: Non-linear Independent Components Estimation. In Yoshua Bengio and Yann LeCun, editors, *3rd International Conference on Learning Representations, ICLR 2015, San Diego, CA, USA, May 7-9, 2015, Workshop Track Proceedings*, 2015. URL <http://arxiv.org/abs/1410.8516>.
- [18] Ivan Kobyzev, Simon Prince, and Marcus Brubaker. Normalizing Flows: An Introduction and Review of Current Methods. *IEEE Transactions on Pattern Analysis and Machine Intelligence*, 2020.
- [19] George Papamakarios, Theo Pavlakou, and Iain Murray. Masked autoregressive flow for density estimation. In *Proceedings of the 31st International Conference on Neural Information Processing Systems*, NIPS’17, page 2335–2344, Red Hook, NY, USA, 2017. Curran Associates Inc. ISBN 9781510860964.

- [20] Volodymyr Mnih, Koray Kavukcuoglu, David Silver, Andrei A Rusu, Joel Veness, Marc G Bellemare, Alex Graves, Martin Riedmiller, Andreas K Fidjeland, Georg Ostrovski, et al. Human-level control through deep reinforcement learning. *nature*, 518(7540):529–533, 2015.
- [21] Aviral Kumar, Aurick Zhou, George Tucker, and Sergey Levine. Conservative q-learning for offline reinforcement learning. *Advances in Neural Information Processing Systems*, 33: 1179–1191, 2020.
- [22] Takuma Seno and Michita Imai. d3rlpy: An offline deep reinforcement learning library. *arXiv preprint arXiv:2111.03788*, 2021.
- [23] Tom Le Paine, Cosmin Paduraru, Andrea Michi, Caglar Gulcehre, Konrad Zolna, Alexander Novikov, Ziyu Wang, and Nando de Freitas. Hyperparameter selection for offline reinforcement learning. *arXiv preprint arXiv:2007.09055*, 2020.
- [24] Greg Brockman, Vicki Cheung, Ludwig Pettersson, Jonas Schneider, John Schulman, Jie Tang, and Wojciech Zaremba. OpenAI Gym. *arXiv preprint arXiv:1606.01540*, 2016.
- [25] Will Grathwohl, Ricky T. Q. Chen, Jesse Bettencourt, Ilya Sutskever, and David Duvenaud. FFJORD: Free-Form Continuous Dynamics for Scalable Reversible Generative Models. In *7th International Conference on Learning Representations, ICLR 2019, New Orleans, LA, USA, May 6-9, 2019*. OpenReview.net, 2019. URL <https://openreview.net/forum?id=rJxgknCcK7>.